



Design of Simple Structure Gas Sensor Based on Hybrid Cladding Photonic Crystal Fiber

Sayed ASADUZZAMAN^{1,*}, Kawsar AHMED¹, Touhid BHUIYAN²

¹Department of Information and Communication Technology, Mawlana Bhashani Science and Technology University, Santosh, Tangail-1902, Bangladesh

²Department of Software Engineering, Daffodil International University, 102-Sukrabad, Mirpur Road, Dhanmondi, Dhaka-1207, Bangladesh

Received: 26.02.2016; Accepted: 09.04.2016

Abstract. A hybrid structure photonic crystal fiber gas sensor is presented in this paper to detect toxic and colorless gases. The guiding properties of proposed structure have been numerically investigated using finite element method (FEM). From the numerical results sensitivity of the proposed structure is enhanced to 15.67%. The Confinement loss or Leakage loss decreased to 1.12×10^{-7} by acquainting an octagonal ring of air holes in the outer cladding. The proposed H-PCF can be used in a wider range of wavelength from $0.8 \mu\text{m}$ to $2 \mu\text{m}$. The proposed structure has significantly lower confinement losses, higher sensitivity and is more flexible for its simplicity compared with early proposed PCFs.

Keywords: Hybrid Photonic Crystal Fiber (H-PCF), Evanescent Field, Gas Sensor, Sensitivity, Finite Element Method and Confinement Loss.

Hibrit Kaplamaları Photonic Kristal Fibere Dayalı Basit Yapılı Gaz Sensörü Tasarımı

Özet. Bir melez yapılı fotonik kristal fiber gaz sensörü, toksik ve renksiz gazları algılamak için, bu çalışmada sunulmuştur. Önerilen yapının yol gösterici özellikleri sayısal sonlu elemanlar metodu (FEM) kullanılarak incelenmiştir. Sayısal sonuçlardan önerilen yapı duyarlılığı %15.67'e yükseltilmiştir. Hapsetme kaybı ya da kaçak kaybı, dış cephe hava deliklerinin sekizgen halka yapısı ile 1.12×10^{-7} değerine düşmüştür. Önerilen H-PCF, $0.8 \mu\text{m}$ ile $2 \mu\text{m}$ dalga boyu aralığında kullanılabilir. Önerilen yapı, daha düşük hapsi kayıpları, yüksek duyarlılık sahibidir ve önceden önerilen PCFs ile karşılaştırıldığında sadeliği için daha esneklerdir.

Anahtar Kelimeler: Hibrit Fotonik Kristal Fiber (H-PCF), Evanescent Alan, Gaz Sensörü, Duyarlılık, Sonlu Elemanlar Metodu ve Hapsetme Kaybı.

1. INTRODUCTION

Photonic crystal fibers (PCFs) consist of periodically arranged air holes in cladding and core run all over the length of fiber [1]. Some unique novel properties of PCFs have drawn the attraction of researchers for its more flexibility than conventional optical fibers. Development of regular or irregular PCF structure helps researchers to achieve more efficiency as well as use it in multipurpose like gas sensing [2-6], chemical sensing [7], bio sensing [8], cancer cell detection [9], medical science [10], and temperature sensing [11-12]. Like different structural shape, geometrical parameters of fiber are also responsible to vary guiding properties [13]. Some different lattice structures like octagonal [14], hexagonal [15], decagonal [16], circular honey comb cladding [17], elliptical [18] were proposed to achieve the better guiding properties of photonic crystal fiber (PCF).

The application of fiber in sensing Hexagonal PCF [3], octagonal PCF [14] and multicore PCF [19], are most popular because of their attractive features and shows lots of peculiar properties such as strong

* Corresponding author. Email address: samonna25@gmail.com

Design of Simple Structure Gas Sensor Based

resistance to electromagnetic interference, good reliable, application of remote monitoring and easy networking etc. [7]. Accurate control of air holes and their periodicity increase the fabrication tolerance [7,11] and also handle index guiding properties like sensitivity, confinement loss etc.

Number of papers has been published to improve the confinement loss and sensitivity. The article of Park et al. [7] was proposed an index-guiding PCF with a high index ring defect in the center for increasing the relative sensitivity and confinement loss simultaneously. The central air hole of proposed PCF was surrounded with a hollow high index $\text{GeO}_2\text{-SiO}_2$ ring defect. A small core surrounding with large air holes shows very large overlap of light [20] in microstructure optical fiber. The octagonal PCF shows better performance than hexagonal PCF for index-guiding properties [21] of microstructure optical fiber. Octagonal PCFs are provided some major attractive feature like lower confinement loss, small effective area and wideband single mode operation comparing to conventional PCFs [22]. Modified OPCFs (innermost layer two air holes are missing and other air holes are elliptical) are more suitable for sensing systems than conventional OPCFs [23]. In 2015, few PCF structures with hybrid cladding were proposed for chemical [24-26] and gas sensing [27, 28].

Md. Selim Habib et al. [29] proposed five rings octagonal photonic crystal fiber structure and reported that pitch variation between two adjacent air holes in the same ring and adjacent rings provided better index guiding properties compare to traditional OPCF. Bo Li et al. [30] proposed an octagonal multicore photonic crystal fiber structure with low confinement loss and good perspective for applications in high power propagation and others fields. Mohammad Nejad et al. [31] proposed two types of OPCF (one is T-OPCF and another is H-OPCF) those are very suitable for near future applications.

The article [7] proposed a new index-guided PCF with a hollow GeO_2 -doped high index ring defect [32, 33] applied in chemical sensing applications to achieve larger evanescent wave interaction efficiency, smaller confinement loss, and smaller splicing loss than prior PCFs simultaneously. This structure reported high sensitivity of 5.09% what has significantly improved from 4.79% of prior structure [3] as well as confinement loss is reduced to 1.25dB/m from 32.4dB/m of prior structure. In [4] provided high sensitivity (10.00% improved compared to prior) and low confinement loss (6.0×10^{-4} times less than prior) by increasing core diameter and decreasing the distance between centers of two adjacent holes. Saeed Olyae et al. [5] proposed an evanescent gas sensor based on modified PCF with high sensitivity and low confinement low. The authors proposed different types of hexagonal PCF structure and reached a maximum sensitivity 13.23% at wavelength $1.33\mu\text{m}$ as well as confinement loss reduced to 3.77×10^{-6} at the same wavelength.

In this paper, a new modified Hybrid Cladding PCF structure (H-PCF) is used to achieve higher relative sensitivity and lower confinement losses than the previous PCF where the proposed Hybrid PCF is consisted with three ring air holes in cladding and the hollow core at the core. In proposed PCF, no

material doping was used and that's why the fabrication cost and as well as complexity is reduced. Also, outermost cladding ring is replaced by an octagonal ring to improve confinement loss and better relative sensitivity is achieved by optimizing the parameters of the proposed simple structure. Finally this paper is introducing an evanescent field gas sensor based on micro structure photonic crystal fiber. A full vector finite element method is applied to analyze the effect of changing different parameters of an index guiding PCF of the proposed structure. And it has also improved sensitivity and confinement loss compare to prior [5] structure.

2. GEOMETRICS OF THE PROPOSED HPCF

Fig 1 shows transverse cross sectional view of the proposed PCF which shows both high sensitivity and low confinement loss along with. The background material is pure silica whose refractive index changes with the wavelength according to the sellmier equation. This simple structure comprises of three rings of air holes. The first two rings of air holes are hexagonal and the outer ring is octagonal. A hollow core is used to centralize the interaction of light in the core region. The diameter of the hollow-core is set to $d_c=2\mu\text{m}$ which has been filled with air. The diameters of the air holes of inner rings, the second ring and the outer ring are denoted as $d_1=2.75\ \mu\text{m}$, $d_2=2.70\ \mu\text{m}$ and $d_3=3.5\ \mu\text{m}$. The hole to hole distance is called the pitch (Λ) of a PCF structure. The distance of the center of the holes between second and third ring assumed as Λ_1 and the distance between the centers of the two adjacent holes of third ring assumed as Λ_2 . Thickness of the two layers of the Perfect Matched Layer (PML) has been set 10% around to meet the factual boundary condition.

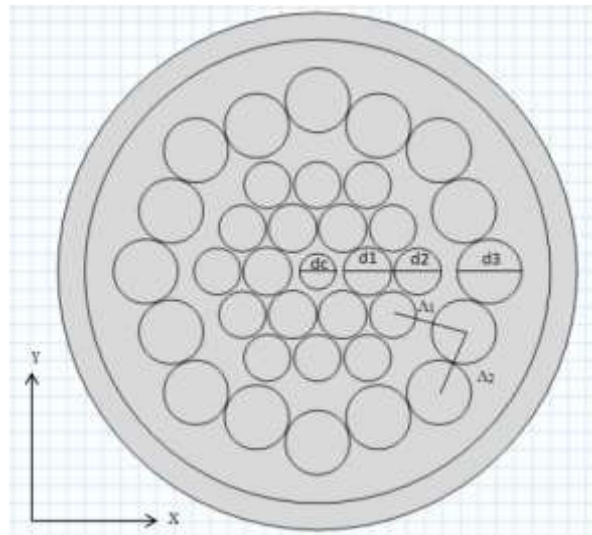


Fig. 1 Transverse Cross-sectional view of proposed structure

3. NUMERICAL METHOD ANALYSIS

To solve the Maxwell's equations finite-element method [FEM] with perfectly matched boundary layers (PML) is utilized because of its reliability [17]. Here is investigated the optical properties of the

Design of Simple Structure Gas Sensor Based

proposed PCF as well as calculated confinement loss and sensitivity, as the goal of this research is to find higher sensitivity and at lower confinement loss simultaneously.

Confinement Loss is one of the most important parameter of the PCF structure. Variations of different parameters are responsible for changing confinement loss such as the number of layers, number of air holes, air hole diameter and the pitch. A small portion of power leakage is unavoidable while light energy passes through a photonic crystal fiber. This leakage of light energy from core to exterior matrix material is known as confinement loss which is related to the attenuation coefficient α of the fundamental mode. The attenuation constant α can be calculated as follow [20]

$$\alpha = 2k_0 \text{Im}[\sqrt{\epsilon}] \quad (1)$$

where, $k_0 = 2\pi/\lambda$ and $\text{Im}[n_{eff}]$ is called as the imaginary part of the refractive index.

Confinement loss (dB/m) L_c is related to the attenuation coefficient α and can be expressed as

$$L_c = 10 \lg e \cdot \alpha = 8.686 \cdot \frac{2\pi}{\lambda} \cdot \text{Im}[n_{eff}] \text{ (dB/m)}$$

The relationship between gas concentration and optical intensity can be expressed according to the Lambert Beers Law and shown in equation (2)

$$I_T(\omega) = I_0(\omega) \exp[-r\alpha(\omega)LC] \quad (2)$$

Where $I_T(\omega)$ and $I_0(\omega)$ are the intensity of transmitted light and incident light respectively, L is path length, C is gas concentration and r is relative sensitivity coefficient.

The relative sensitivity coefficient can be derived using below formula and denoted by equation (3)

$$r = \frac{n_s}{\text{Re}[n_{eff}]} f \quad (3)$$

Where, n_s is the refractive index of the absorbing material and $\text{Re}[n_{eff}]$ is the real part of effective refractive index. f is the ratio of optical power of the air holes to the total power.

According to the Poynting's theorem f can be expressed as

$$f = \frac{\int_{\text{sample}} \text{Re}(E_x H_y - E_y H_x) dx dy}{\int_{\text{total}} \text{Re}(E_x H_y - E_y H_x) dx dy} \quad (4)$$

Where, E_x and H_x are transverse electric field and magnetic field, E_y and H_y are longitudinal electric field and magnetic field. Using finite-element method (FEM) we obtained the mode field pattern E_x , H_x , E_y , H_y and effective index n_{eff} with COMSOL Multiphysics 4.2.

4. RESULT AND DISCUSSION

The relationships among wavelength, sensitivity, confinement loss, hollow core, first layer diameter, second layer diameter and modal intensity are analyzed in this section. Resultant confinement loss and sensitivity are also described for the variation of different PCF properties.

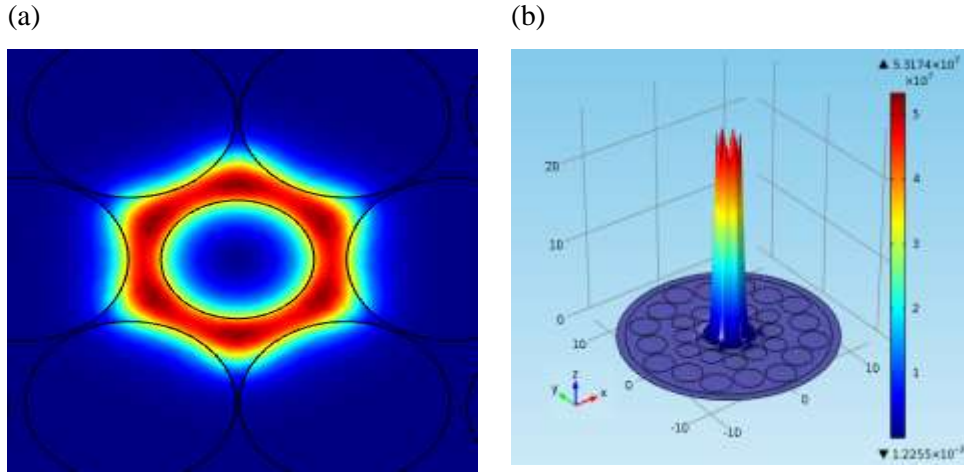


Fig. 2 (a) Two dimensional end-face electric field distribution of the fundamental mode. (b) three dimensional electric field distribution of the fundamental mode.

In the core region the fundamental mode in the proposed PCF is tightly confined which has been shown in the Fig. 2. From the figure it is examined that the electric field distribution is uniform around the hollow core. Fig. 3 represents the three dimensional field distribution of the fundamental mode through the Z-axis.

The comparison of relative refractive index and wavelength are shown in the Fig. 3 for varying hollow core $dc=1.8 \mu\text{m}$, $dc=2.0 \mu\text{m}$ and $dc=2.2 \mu\text{m}$. From the figure it is clear that for all cases the refractive index decreases linearly with the increase of wavelength. It seems that the relation of wavelength and refractive index is anti-proportional.

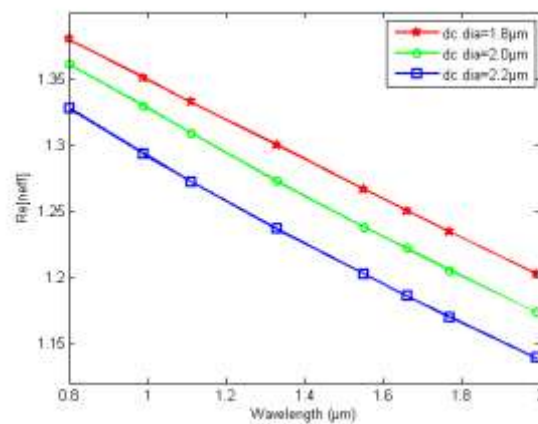


Fig. 3 variation of the real part of effective refractive index as a function of wavelength for different hollow core $dc=1.8 \mu\text{m}$, $dc=2.0 \mu\text{m}$ and $dc=2.2 \mu\text{m}$

Design of Simple Structure Gas Sensor Based

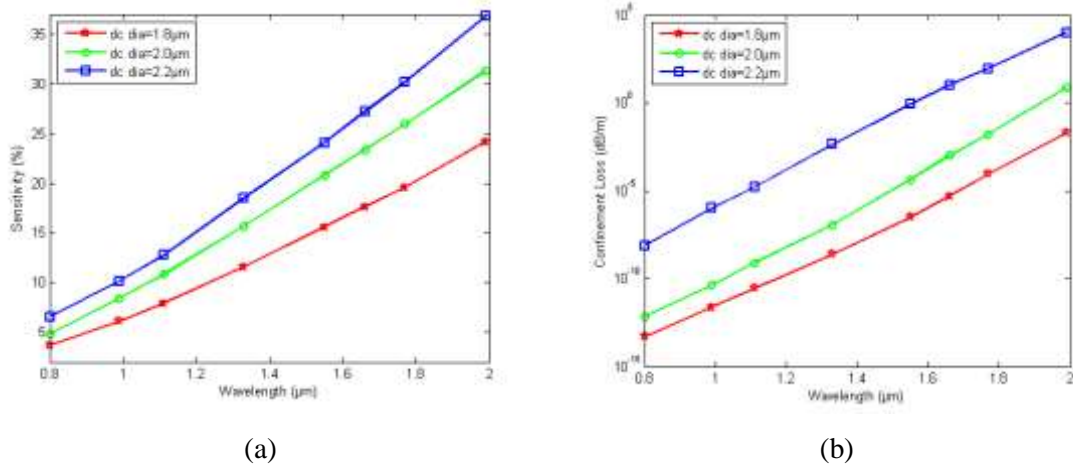


Fig. 4 (a) Sensitivity versus wavelength and (b) confinement loss versus wavelength by varying hollow core $d_c=1.8 \mu\text{m}$, $d_c=2.0 \mu\text{m}$ and $d_c=2.2 \mu\text{m}$

Fig. 4 shows the investigation impact of changing of hollow core diameter on relative sensitivity and confinement loss. Both the relative sensitivity and confinement loss increases according with the increasing of the core diameter which has been shown in the figure when $d_1=2.75 \mu\text{m}$, $d_2=2.70 \mu\text{m}$ and $d_3=3.50 \mu\text{m}$. The optimized value of $d_c=2.0 \mu\text{m}$ was set due to both high relative sensitivity and lower confinement loss. Although the higher diameter of $d_c=2.2 \mu\text{m}$ shows better sensitivity but it was eliminated due to avoid collision of air holes.

Fig. 5 depicts significant impact on the PCF for sensitivity with different diameter of the air hole of the nearest ring to the core. Both relative sensitivity and confinement loss increases with the increasing of inner ring diameters when the other optimized parameters $d_c=2.0 \mu\text{m}$, $d_2=2.70 \mu\text{m}$ and $d_3=3.50 \mu\text{m}$ were constant.

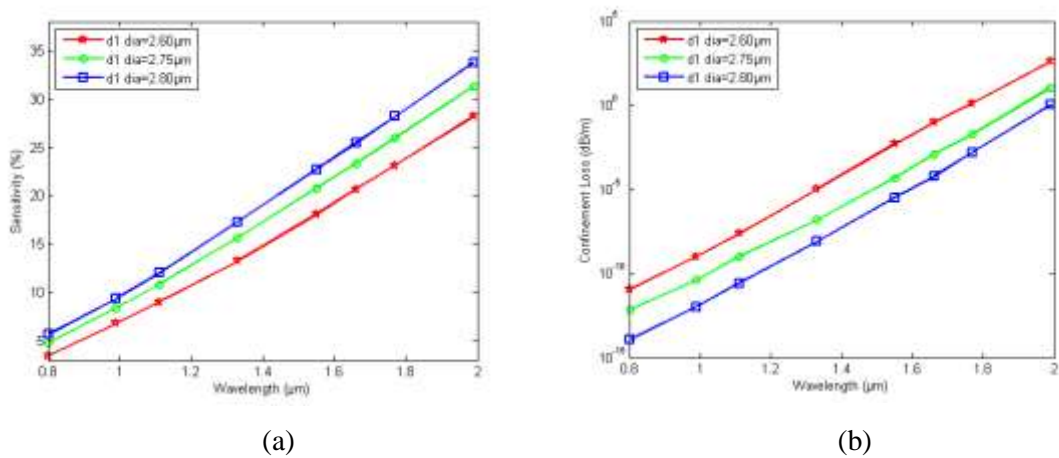


Fig. 5 (a) Relative sensitivity versus Wavelength and (b) Confinement loss versus Wavelength for $d_1=2.60 \mu\text{m}$, $d_1=2.75 \mu\text{m}$ and $d_1=2.80 \mu\text{m}$ when $d_c=2.0 \mu\text{m}$, $d_2=2.70 \mu\text{m}$ and $d_3=3.50 \mu\text{m}$ were optimized.

The impact of change in relative sensitivity and confinement loss with the change of outer ring of sir holes has been illustrated in Fig. 6. From the figure it is clear that the relative sensitivity remains same but the confinement loss varies with the wavelength. So it can be demonstrate that the outer ring of the PCF has a great impact on confinement loss. The outer ring varies while the optimized parameters $d_c=2.0\mu\text{m}$, $d_1=2.60\mu\text{m}$, $d_2=2.70\mu\text{m}$ remains constant. The confinement loss increases gradually with the wavelength but it is not linear in nature.

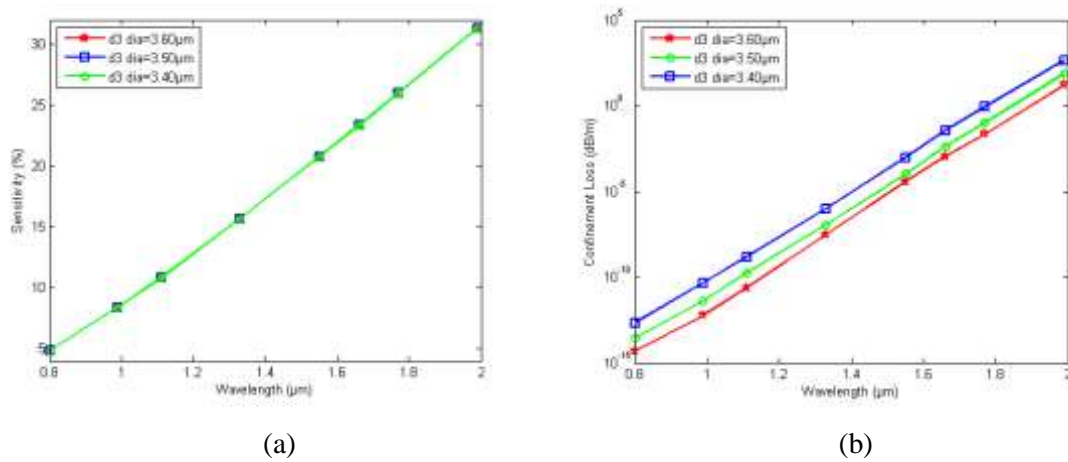


Fig 6 (a) Relative sensitivity versus Wavelength and (b) Confinement loss versus Wavelength for $d_3=3.60\mu\text{m}$, $d_3=3.50\mu\text{m}$ and $d_3=3.40\mu\text{m}$ when $d_c=2.0\mu\text{m}$, $d_1=2.75\mu\text{m}$ and $d_2=2.70\mu\text{m}$ were optimized.

Fig. 7 shows the comparison of Relative sensitivity and confinement loss between the prior and the proposed PCFs. From the both figures it is clear that in the proposed PCF the relative sensitivity is greatly enhanced and also shows a low confinement loss varying with the wavelength which is much better than the prior PCF.

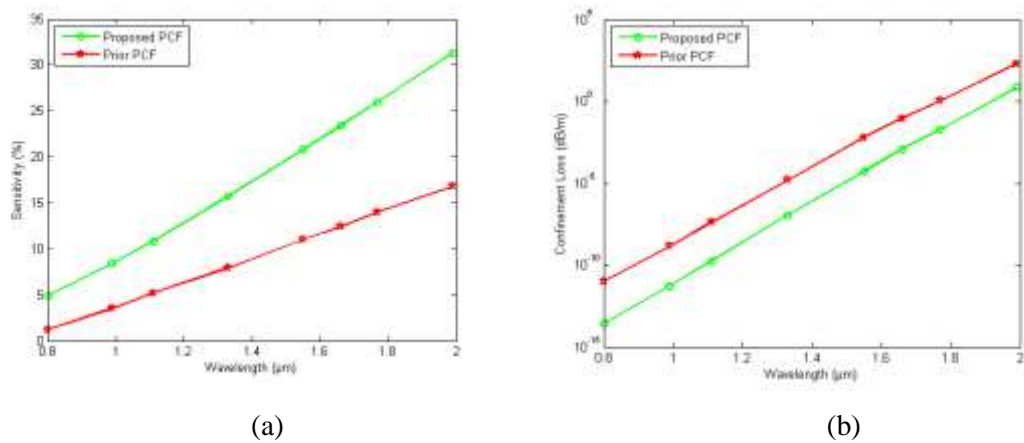


Fig. 7 (a) Relative sensitivity versus Wavelength and (b) Confinement loss versus Wavelength of proposed and prior PCF structures.

Design of Simple Structure Gas Sensor Based

The values of the relative sensitivity and confinement loss among the proposed optimum H-PCF and the different global parameters have been shown in Table 1. The table describes the optimization of the parameters and its better consequences. The proposed PCF has been analyzed at the wider range of wavelength of 0.8 μ m to 2 μ m where a huge number of absorption line relies. The proposed H-PCF can sense the colorless and toxic gases like (Ammonia, Carbondioxide, Mithene etc) within the absorption line of the relevant gases.

Table 1 Values of Relative Sensitivity and Confinement loss among the various global parameters and optimized values of proposed H-PCF.

Change in Parameters (%)	Sensitivity (r%)	Con. Loss (dB/m)
+10	16.01%	2.46×10^{-3}
+5	15.98%	2.94×10^{-4}
Optimum	15.67%	1.12×10^{-7}
-5	33.12%	2.09×10^{-7}
-10	32.01%	3.66×10^{-7}

Lastly, the proposed PCF sensor shows simplicity than any other PCF structure which have been proposed before. The prior PCF gas sensors are very complex in geometry. It introduced that sensitivity increases for replacement of circular air holes by hexagonal air holes at first ring. Increment of sensitivity is 9.9% to 13.23% at wavelength 1.33 μ m where the proposed structure shows 15.67%. As like as sensitivity the proposed structure also reduces confinement loss 1.12×10^{-7} from 3.77×10^{-6} . With a hollow core and the combination of hexagonal and octagonal geometry, it brings more unique than any other optical gas sensors and chemical sensors. Without using doping the proposed H-OPCF shows high sensitivity and low confinement loss simultaneously. The background silica is surrounded with only 41 air holes, arranged in a very simple geometric structure which is easy to fabricate and also results in lower cost for manufacturing and highly applicable in sensing systems. Due to the advancement of nanotechnology the Proposed PCF can be fabricated by the modern fabrication techniques like sol-gel [29] and selective-filling technique [30]. By sol-gel Technique any type of PCF with different hole size can be fabricated.

5. CONCLUSIONS

In conclusion, a simple Hybrid PCF structural gas sensor based on the index-guiding PCF with hollow core is designed. Two sensing properties such as sensitivity and confinement loss have been investigated on proposed Hybrid PCF at different wavelength. The proposed Hybrid PCF successfully obtained higher sensitivity and lower confinement loss simultaneously. To achieve more sensitivity, innermost air holes diameter in first layers are increased and designed in circular as well as second layer. The outermost layer among three layers is designed in circular also for reducing confinement loss. At wavelength $\lambda=1.33\mu$ m, the Methane absorption line is enhanced to the relative sensitivity value of

15.67% but in early published index-guiding PCF was 13.23% as well as confinement loss has been reduced to 1.12×10^{-7} from 3.77×10^{-6} . We mostly hopeful that the proposed Hybrid PCF will be helpful for gas sensing as well as chemical sensing system applications and successfully overcome the critical trade-off between two index-guiding properties like sensitivity and confinement loss.

Acknowledgements

The authors are grateful who participated in this research.

REFERENCES

1. Russell P, 2003. Photonic crystal fibers. *Science*, 299 :358-362.
2. Xin G, Ying L, Hai W, Jia H, Chen H, Juan M, Lou Z, 2014. Research on Distributed Gas Detection Based on Hollow-core Photonic Crystal Fiber. *Sensors & Transducers*, 174:14-20.
3. Yu X, Sun Y, Ren G, Shum, P, Ngo P, and Kwok Y, 2008. Evanescent Field Absorption Sensor Using a Pure-Silica Defected-Core Photonic Crystal Fiber, *Photonic Technology Letter*, 20:336–338.
4. Olyee S and Naragi A, 2013. Design and Optimization of Index-Guiding Photonic Crystal Fiber Gas Sensor, *Photonic Sensors*, 3:131–136.
5. Olyae S, Naraghia A and Ahmadil, 2014. High sensitivity evanescent-field gas sensor based on modified photonic crystal fiber for gas condensate and air pollution monitoring. *Optik*, 125: 596–600.
6. Dash J and Jha R, 2014. Graphene-Based Birefringent Photonic Crystal Fiber Sensor Using Surface Plasmon Resonance. *IEEE Photonics Technology Letters*, 26:1092-1095.
7. Park J, Lee S, Kim S and Oh K, 2011. Enhancement of chemical sensing capability in a photonic crystal fiber with a hollow high index ring defect at the center. *Optical Express*, 19: 1921-1929.
8. Akowuah E, Gorman T, Ademgil H, Haxha S, Robinson G and Oliver J, 2012. Numerical analysis of a photonic crystal fiber for biosensing applications. *IEEE J. Quantum Electron.*, 48: 1403–1410.
9. Sharan P, Bharadwaj S, Gudagunti F and Deshmukh P, 2014. Design and Modelling of Photonic Sensor for Cancer Cell Detection, *International Conference on the Impact of E-Technology on US (IMPETUS)*, IEEE Computer Society: 20-24.
10. Hossain M and Maniruzzaman M. Prospect of Photonic Crystal Fiber (PCF) In Medical Science. *Proceedings of 4th Global Engineering, Science and Technology Conference*, BIAM Foundation, Dhaka, Bangladesh, (2013) p. 1-5.
11. Olyae S and Dehghani A, 2012. High resolution and wide dynamic range pressure sensor based on two-dimensional photonic crystal. *Photonic Sensors*, 2: 92–96.
12. Wua D, Zhao Y and Hu H, 2014. Experimental research on FLM temperature sensor with anethanol-filled photonic crystal fiber. *Sensors and Actuators A*, 209: 62–67.
13. Xu Z, Duan K, Liu Z, Wang Y, and Zhao W, 2009. Numerical analyses of splice losses of photonic crystal fibers. *Optics Communications*, 282: 4527–4531.
14. Habib M, Habib M, Razzak S, and Hossain M, 2013. Proposal for highly birefringent broadband dispersion compensating octagonal photonic crystal fiber, *Optical Fiber Technology*, 19: 461–467.
15. Begum F, Namihira Y, Razzak S, Kaijage S, Hai N, Kinjo T, Miyagi K, and Zou N, 2009. Design and analysis of novel highly nonlinear photonic crystal fibers with ultra-flattened chromatic dispersion. *Optics communications*, 282:1416–1421.
16. Razzak S, Namihira Y, Khan M, Begum F, and Kaijage S, 2007. Guiding Properties of a Decagonal Photonic Crystal Fiber. *Journal of Microwaves, Optoelectronics and Electromagnetic Application*, 6.
17. Hou Y, Fan F, Jiang Z, Wang X, and Chang S. Highly birefringent polymer terahertz fiber with honeycomb cladding. *Optik-International Journal for Light and Electron Optics*, 124: 3095–3098.
18. Hao R, Li Z, Sun G, Niu L, and Sun Y, 2013. Analysis on photonic crystal fibers with circular air holes in elliptical configuration. *Optical Fiber Technology*, 19: 363–368.

19. Baili A, Cherif R, and Zghal M, 2014. New design of multicore nonlinear photonic crystal fiber for mid-IR supercontinuum generation, SPIE Photonics Europe: 91280A–91280A.
20. Monro T, Smith S, Schartner S, Francois A, Heng S, Ebendorff H, Afshar S, 2010. Sensing with suspended-core optical fibers. *Optical Fiber Technology*, 16 :343–356.
21. Guan J, 2008. Finite Element Analysis of propagation Characteristics for an Octagonal Photonic Crystal Fiber (O-PCF). *Proc. of SPIE*, 7134 :71342P (1-7).
22. Chiang J, and Wu T, 2006. Analysis of propagation characteristics for an octagonal photonic crystal fiber (O-PCF). *Optical Communication*, 258 :170-176.
23. Habib M, Habib M, Razzak S and Hossain M, 2013. Proposal for highly birefringent broadband dispersion compensating octagonal photonic crystal fiber, *Optical Fiber Technology*, 19: 461-467.
24. S. Asaduzzaman, M. F. H. Arif, K. Ahmed, and P. Dhar, “Highly sensitive simple structure circular photonic crystal fiber based chemical sensor,” in 2015 IEEE International WIE Conference on Electrical and Computer Engineering (WIECON-ECE), 2015, pp. 151–154.
25. K. Ahmed, S. Asaduzzaman, and F. H. Arif, “Numerical analysis of O-PCF structure for sensing applications with high relative sensitivity,” in *Electrical Information and Communication Technology (EICT)*, 2015 2nd International Conference on, 2015, pp. 254–258.
26. S. Asaduzzaman, M. Kawsar Ahmed, F. H. Arif, and M. Morshed, “Application of Microarray-core Based Modified Photonic Crystal Fiber in Chemical Sensing.”
27. M. Morshed, M. F. H. Arif, S. Asaduzzaman, and K. Ahmed, “Design and characterization of photonic crystal fiber for sensing applications,” *European Scientific Journal*, vol. 11, no. 12, 2015.
28. M. Morshed, S. Asaduzzaman, M. Faizul Huq Arif, and K. Ahmed, “Proposal of simple gas sensor based on micro structure optical fiber,” in *Electrical Engineering and Information Communication Technology (ICEEICT)*, 2015 International Conference on, 2015, pp. 1–5.
29. Habib M, Habib M, Hasan M and Razzak S, 2013. Tailoring polarization maintaining broadband residual dispersion compensating octagonal photonic crystal fibers, *Optical Engg*, 52: 116111(1)-116111(8).
30. Li B, Zhou G, Xia C, Liu H and Hou Z, 2014. Analysis of supermode and structural characteris of octagonal multicore photonic crystal fiber with large effective area and low confinement loss. *Optical Engg*, 53 :056114 1-6.
31. Nejad S, Aliramezani M and Pourmahyabadi M. Novel Design of an Octagonal Photonic Crystal Fiber with Ultra-Flattened Dispersion and Ultra-Low Loss, *IEEE 3rd International Conference On Broadband Communications, Information Technology & Biomedical Applications (2008)* p.221-226.
32. Kim S, Paek U and Oh K, 2005. New defect design in index guiding holey fiber for uniform birefringence and negative flat dispersion over a wide spectral range. *Opt. Express*, 13: 6039–6050.
33. Dash J and Jha R, 2014, Graphene-Based Birefringent Photonic Crystal Fiber Sensor Using Surface Plasmon Resonance. *IEEE Photo Tech Let*, 26: 1092-1095.
34. Bise R and Trevor D. Sol-gel derived microstructured fiber: Fabrication and characterization. *Optical Fiber Communications Conf.(OFC)*, (2005).
35. Huang Y, Xu Y, and Yariv A, 2004. Fabrication of functional microstructured optical fibers through a selective-filling technique. *Applied Physics Letters*, 85: 5182–5184, 2004.